Effect of the Missing Indonesian Throughflow in the Fine Resolution Antarctic Model

JOACHIM RIBBE AND MATTHIAS TOMCZAK

School of Earth Sciences, Flinders University of South Australia, Adelaide, Australia

(Manuscript received 20 December 1995, in final form 3 September 1996)

ABSTRACT

South of Tasmania, the Fine Resolution Antarctic Model (FRAM) shows a narrow band of westward flow in the surface layer. The authors argue that this is caused by the closure of the Indonesian passage in FRAM. This is supported by numerical experiments carried out by Hirst and Godfrey and by recent radiocarbon observations in the Great Australian Bight (Ribbe et al.). The FRAM surface temperature and salinity distribution exhibits distinct anomalies in the southeast Indian Ocean, in good agreement with anomalies observed in the Hirst and Godfrey model. Indonesian Throughflow water advects heat into the Indian Ocean; its absence in FRAM results in a lack of thermal energy to warm the Indian Ocean in the model. The surface salinity anomaly is most likely caused by an overestimated Ekman transport. The weakened heat and salinity transport in FRAM restricts surface convection in the midlatitude region to approximately 350 m.

The effect of the Indonesian Throughflow closure in FRAM is even more dramatic for the circulation around Australia and Tasmania. Hirst and Godfrey's results suggest that in the case of an open Indonesian passage, the flow in the surface layer is eastward, that is, from the Indian to the Pacific Ocean. Preliminary analysis of radiocarbon observations from the Great Australian Bight supports this, showing a better correlation with Indian Ocean data than Pacific Ocean data. FRAM shows westward flow, inconsistent with these observations.

1. Introduction

The Fine Resolution Antarctic Model (FRAM) is an eddy-resolving model of the circulation of the Southern Ocean. The northern boundary of the model is located at 24°S where the model temperature and salinity is relaxed to Levitus (1982) climatology in all levels that are characterized by inflow. In regions where velocity is directed out of the model region, the boundary temperature and salinity values are determined from inside the model domain (Stevens 1991). Flow across the boundary is allowed, but the net flux across each individual ocean basin is zero. This excludes the possibility of net southward transport in the Indian Ocean from the Indonesian Throughflow (and, likewise, net northward transport in the Pacific Ocean).

In this paper we investigate the effect of the missing throughflow upon sea surface temperature (SST), sea surface salinity (SSS), and the flow pattern in the surface layer of the southeast Indian Ocean. We demonstrate that the absence of the throughflow causes temperature anomalies, weakens convection in regions of Subantarctic Mode Water formation, and possibly results in a reversal of the surface flow around the southeast corner of the Australian continent. We compare the FRAM data with results from the model of Hirst and Godfrey (1993) and with conclusions that can be drawn from radiocarbon observations in the Great Australian Bight (Ribbe et al. 1996).

The Indonesian Throughflow is an important link in the global thermohaline circulation (Broecker 1991), allowing flow from the Pacific Ocean into the Indian Ocean north of Australia. It constitutes one of the possible return pathways for North Atlantic Deep Water (NADW), which upwells in the Southern Ocean and into the permanent thermocline of Pacific Ocean. This ''warm water route,'' in which the return flow is variably estimated between 2 and 16 Sv [Sv $\equiv 10^6$ m^3 s^{-1}, Godfrey (1996)], is complemented by the ''deep water route'' from the Pacific into the Atlantic Ocean through the Drake Passage (Rintoul 1991). A recent reappraisal of the global thermohaline circulation by Schmitz (1995) presents a synthesis of the available information into a somewhat more complex four-layered system. However, in all concepts of the global thermohaline circulation the Indonesian Passage remains a main pathway for the exchange of thermocline water between the Pacific and Indian Oceans.

Several authors (e.g., The FRAM Group 1991; Saunders and Thompson 1993; Stevens and Killworth 1992; Killworth 1992; Thompson 1993; Quartly and Srokosz 1993; Döös and Webb 1994; Stevens and Thompson 1994; Feron 1995; Grose et al. 1995; Lutjeharms and Webb 1995; Wadley and Bigg 1994) have analyzed FRAM model data. A detailed description of FRAM

Corresponding author address: Joachim Ribbe, The Flinders University of SA, School of Earth Sciences, G.P.O. Box 2100, Adelaide, 5001 SA, Australia.
E-mail: mojr@gaea.es.flinders.edu.au

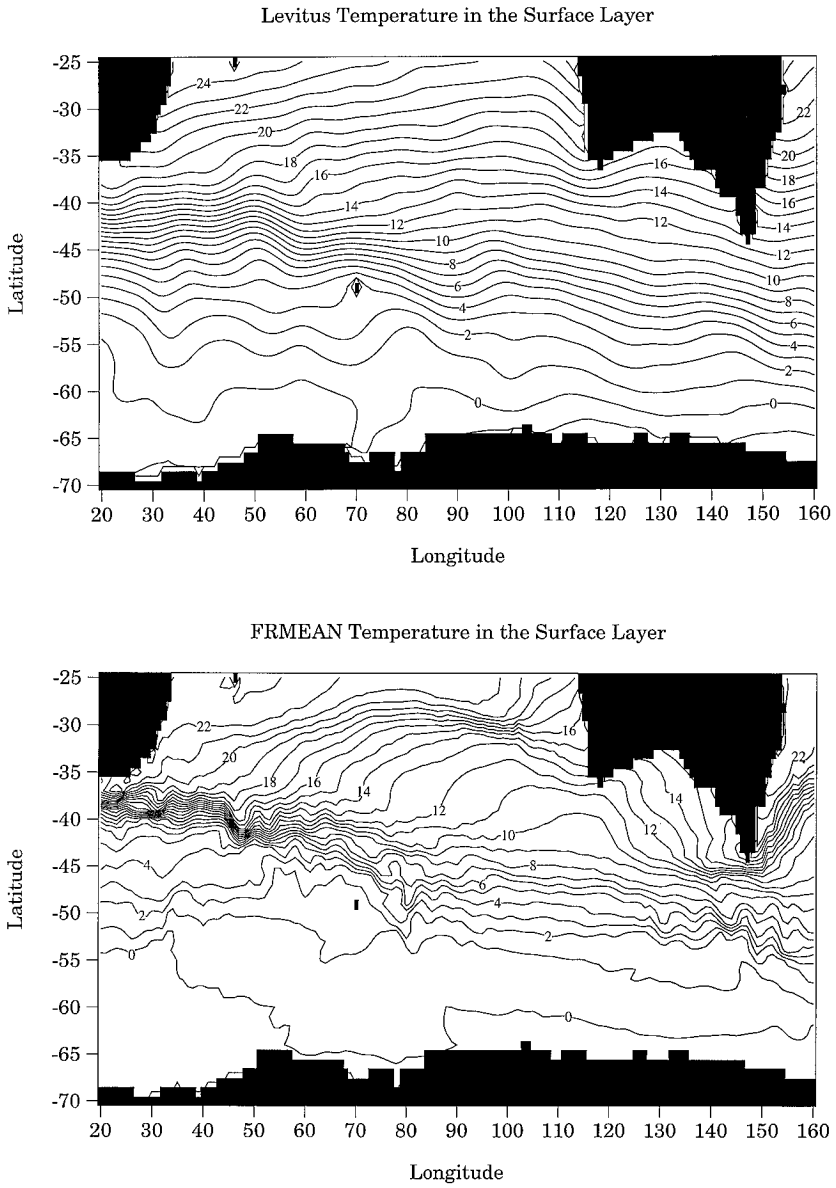

FIG. 1. Sea surface temperature, contoured in 1°C intervals. (a) Levitus (1982) annual mean climatology; note the slope of the isotherms west of Australia indicating the southward flowing Leeuwin Current. (b) FRAM mean SST; note the difference in the slope of the isotherms west of Australia against (a). (c) The difference (a) − (b). Dark shaded areas indicate FRAM heat flux into the ocean.

can be found in this literature. Analysis so far indicates good agreement between the observational and model databases. Only Wadley and Bigg (1994) identified a serious problem within the deep ocean circulation resolved by FRAM. Abyssal flow between the Brazil and Argentine Basins is incorrectly resolved due to topographic smoothing of the Vema Channel.

FRAM was primarily developed to investigate the particular dynamics of the Southern Ocean, characterized by high mesoscale eddy activity. The model was integrated for 16 years only, not allowing for large-scale changes in the distribution of temperature and salinity. Bottom, deep, intermediate, and mode waters, originally prescribed by the Levitus (1982) climatology, are still present in the FRAM dataset at the end of the integration (Webb et al. 1991). Although a large component of the observed dynamics and property distribution within the Southern Ocean is wind driven, interaction with the thermohaline component of the large-scale dynamics does occur. How much a possible misrepresentation of the thermohaline structure affects the overall dynamics within FRAM remains to be investigated.

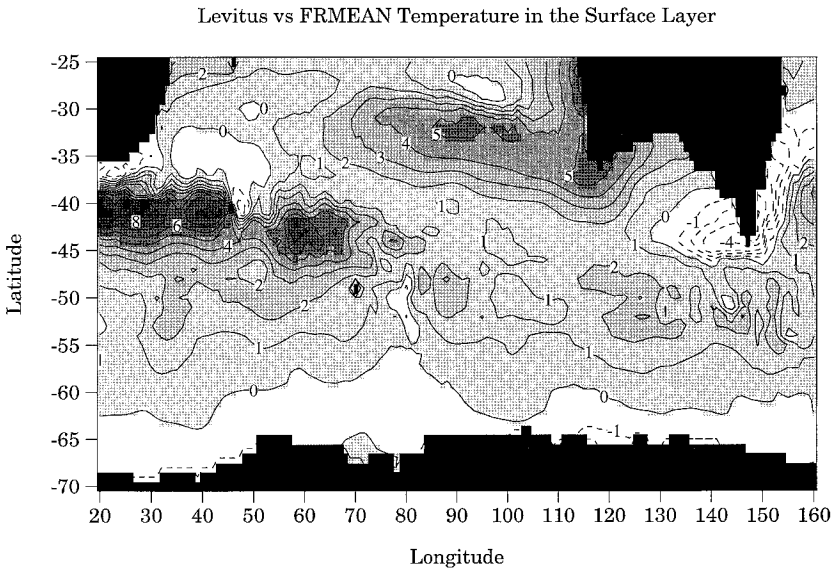

FIG. 1. (*Continued*)

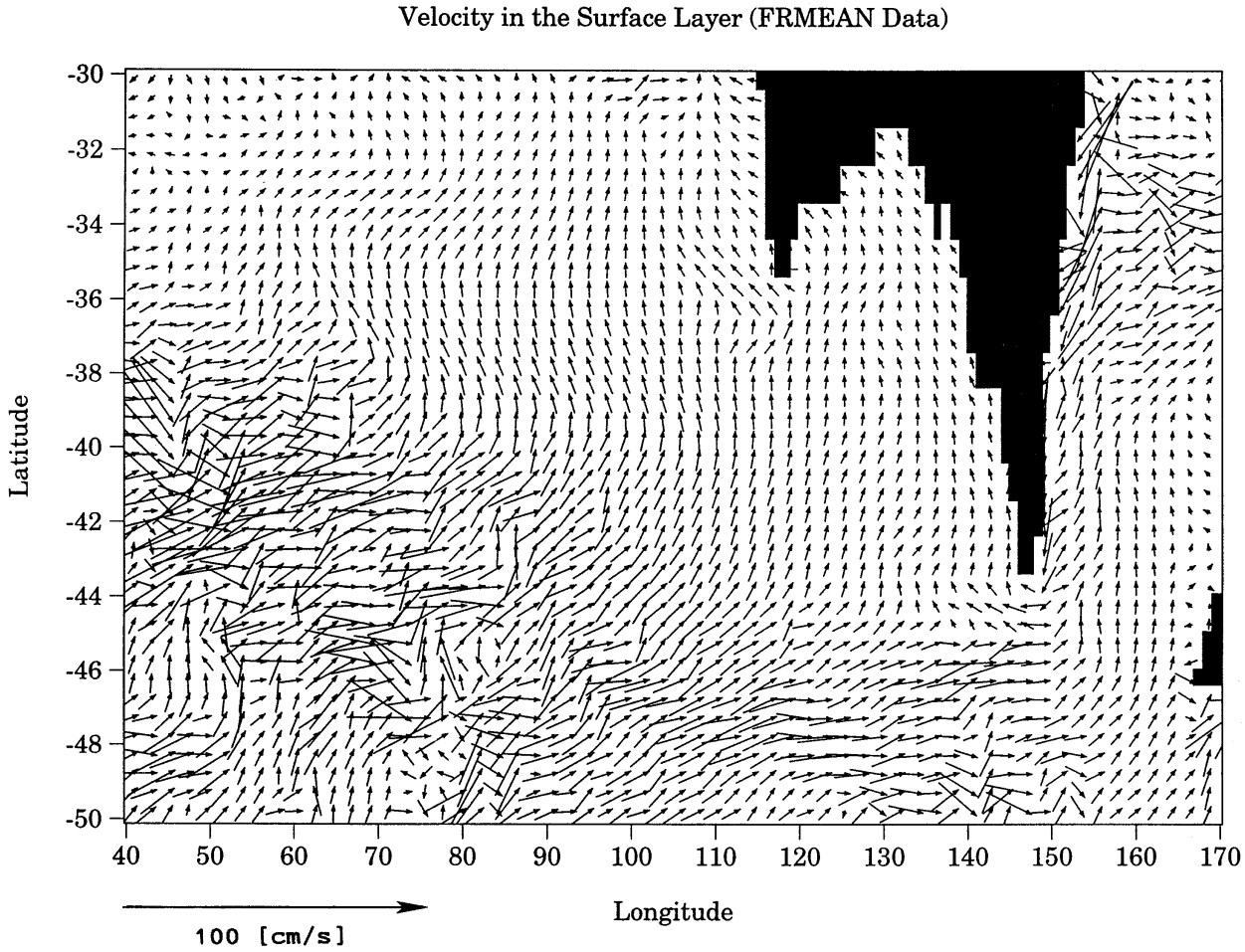

FIG. 2. Velocity in the surface layer of the FRAM. Velocity vectors are not shown for all grid points to reduce the FRAM data density. Note the absence of any southward flow along the west Australian coast.

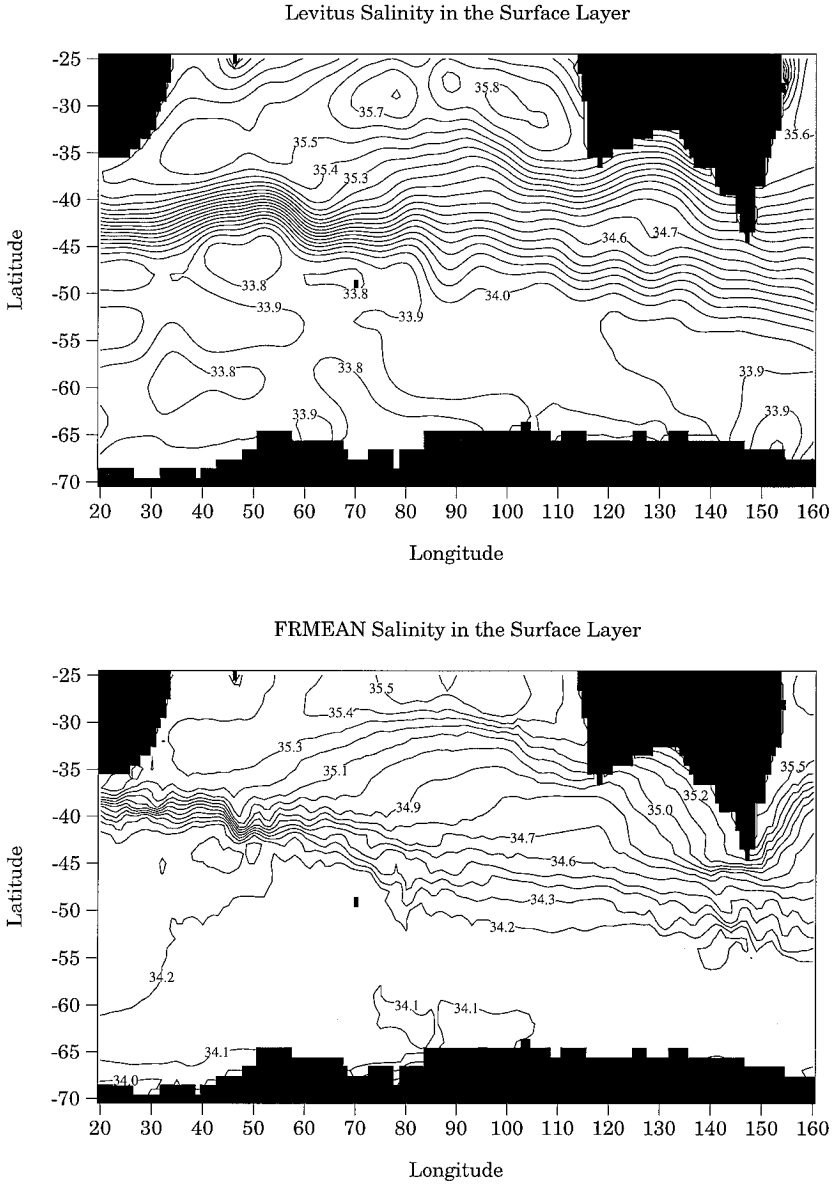

FIG. 3. Sea surface salinity, contoured at 0.1 intervals. (a) Levitus annual mean climatology; note the maximum in the center of the Indian Ocean subtropical gyre. (b) FRAM mean SSS. (c) The difference (a)–(b).

A major consequence of the Indonesian passage is the Leeuwin Current along the West Australian coast (e.g., Tomczak and Godfrey 1994). The Leeuwin Current is a narrow current along the continental shelf and therefore can be considered a somewhat localized phenomenon, and its absence in FRAM could be considered a minor irritation. We intend to show here that the absence of the Indonesian Throughflow in FRAM is not restricted to the suppression of the Leeuwin Current but has much further reaching implications for the property distribution and dynamics. It causes anomalies in the temperature and salinity fields, and a possible reversal of the surface flow from the Great Australian Bight into the Tasman Sea seen in observations to westward flow in FRAM.

2. Results

We used the FRMEAN dataset supplied by the FRAM group for our analysis of the FRAM temperature and salinity distribution. The dataset was obtained as an average of the 72 monthly datasets from FRAM years 11–16 (B. de Cuevas 1995, personal communication). In the following, the surface temperature distribution is discussed first, followed by the surface salinity distribution and the distribution of convection in midlatitu-

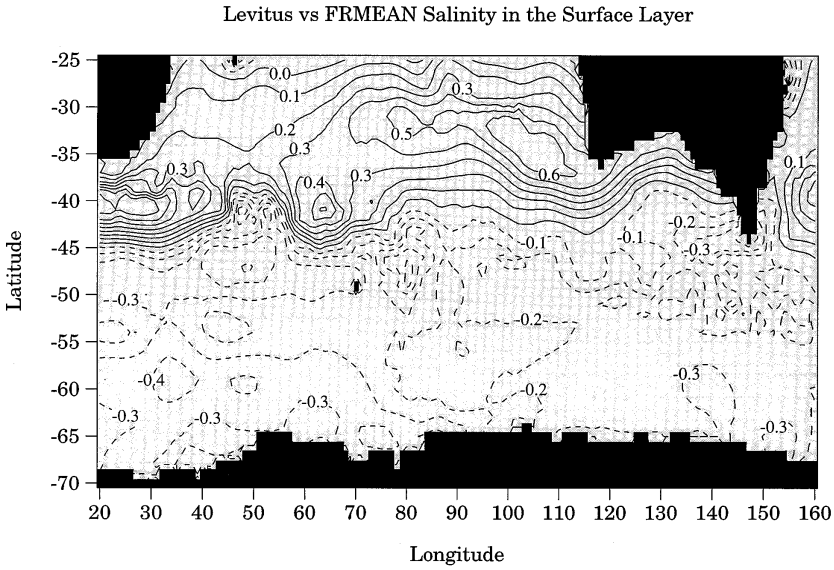

FIG. 3. (*Continued*)

dinal regions; all are compared with the Levitus (1982) annual mean climatology in turn.

a. Temperature

Figure 1 shows the temperature distribution for the Indian Ocean surface layer south of 24°S from the Levitus annual mean climatology (a) and from FRAM (b); the last panel gives the difference between the two datasets (c). Regions of large differences are found in the Agulhas Current (AC) and Retroflection domain, west of Australia and north of the Subantarctic Front (SAF), and south of Tasmania extending from the Pacific Ocean into the Great Australian Bight westward to approximately 130°E. The anomaly associated with the domain of the AC and Retroflection is most likely a result of the particular nature of how FRAM resolves mesoscale activity and maintains frontal gradients that are heavily smoothed in the Levitus dataset. In this area, FRAM is generally colder than the Levitus climatology. This feature is not limited to the climatological mean; Lutjeharms and Webb (1995) show a much colder FRAM in a comparison with quasi-synoptic data (their Fig. 7), not only in the surface layer but extending into deeper layers as well.

The following discussion concentrates on the two larger scale features in the vicinity of the Australian continent. West of Australia, the FRAM SST is significantly lower than observed in the climatology. South of Tasmania, FRAM SST is higher. This pattern is consistent with results of Hirst and Godfrey (1993), who carried out two experiments with a global ocean circulation model to investigate the effect of the Indonesian Throughflow on the global oceanic circulation. In their experiment 1, the Indonesian passage was open, allowing for exchange between the Pacific Ocean and Indian Ocean. In their experiment 2, the passage was closed. With a closed passage less heat is transported into the Indian Ocean. Temperatures are lower, near the surface and in deeper layers as well. The SST anomaly is largest west of Australia. This contrasts with an increased SST for most of the Pacific Ocean extending into the Tasman Sea and the Great Australian Bight.

A similar result to that of Hirst and Godfrey (1993) was recently obtained by K. Szymanska and J.A.T. Bye (1995, personal communication). In their model of the Southern Hemisphere circulation, the Indonesian Throughflow was reduced from 10 to 0 Sv. This resulted in temperature anomalies corresponding to those seen in Hirst and Godfrey's (1993) experiments 1 and 2 as well as in our comparison of Levitus mean annual climatology with FRAM data.

Keeping in mind that FRAM does not include the Indonesian Throughflow, we conclude from the work by Hirst and Godfrey (1993) that the omission of a throughflow domain north of Australia does have a significant impact upon FRAM characteristics. The resulting lowering of SST is not restricted to the Leeuwin Current along the West Australian coast but occurs on a much larger scale.

We are able to derive some more definite conclusions about a possible misrepresentation of the heat flux in FRAM by interpreting Fig. 1c as a heat flux map. This in turn can be compared to a heat flux climatology based upon observations (e.g., Oberhuber 1988). During the integration period of years 11–16, FRAM SST was relaxed to Levitus (1982) climatology. At the ocean surface, the Haney (1971) boundary condition was used that defines the heat flux Q across the air–sea interface with: $Q = \tau^{-1}(T_B - T)$ [T_B = prescribed Levitus (1982) surface value, T = model ocean temperature, τ = re-

laxation timescale]. During the initial spinup of the model, a relaxation timescale of $\tau = 360$ days (The FRAM Group 1991) is used throughout the model domain. The relaxation is chosen to be weak so that FRAM develops mesoscale and other features of the Southern Ocean circulation realistically. Later on, the model runs free from relaxation with the exemption of the surface layer where a timescale of only $\tau = 30$ days was used during the integration period of years 11–16 (B. de Cuevas 1996, personal communication). The timescale of $\tau = 30$ days corresponds to an effective Haney flux coefficient $K \sim c_p \rho H \tau^{-1}$ in the range of about 34 W m^{-2} °C^{-1} [$c_p = 4200$ J kg^{-1} °C^{-1} (specific heat capacity), $\rho = 1025$ kg m^{-3} (density of ocean water), $H = 20.7$ m (thickness of model surface layer)]. This effective Haney flux coefficient used in FRAM is equivalent to that used in many other modeling studies (e.g., Cai and Godfrey 1995).

The temperature differences shown in Fig. 1c are larger than 5°C for the southeast Indian Ocean between approximately 30°–40°S and west of Australia. This amounts to a FRAM heat flux into the ocean of larger than 170 W m^{-2} using the effective flux coefficient in the order of 34 W m^{-2} °C^{-1}. In contrast, the Oberhuber (1988) data indicate an oceanic heat loss for this region of larger than 60 W m^{-2}. South of Tasman, FRAM indicates a heat loss of around 136 W m^{-2}, which corresponds to Oberhuber's (1988) value of around 20 W m^{-2}. For these two locations of the World Ocean the Oberhuber (1988) data are reasonably accurate. Based upon the heat flux interpretation of our Fig. 1c, we are able to conclude definitely that FRAM is not representing the heat flux correctly for most of the southeast Indian Ocean between approximately 30°–40°S, and for the ocean south of Tasmania. The heat flux interpretation supports our idea that the missing Indonesian Throughflow and the associated lack of heat transport through the passage into the Indian Ocean is the most likely cause for the discrepancies.

Figure 1c also shows a negative SST anomaly in the southwestern Tasman Sea extending into the Great Australian Bight to approximately 130°E. This is again consistent with the effect of closing the throughflow. Hirst and Godfrey (1993) highlight the fact that in the case of a closed Indonesian passage a complete reversal of the circulation in the Tasman Sea was observed. The velocity field for the surface layer in FRAM, shown in Fig. 2, shows strong westward flow around the southeastern part of Australia and a northward flow into the Great Australian Bight, a flow pattern possible consistent with a closed Indonesian Throughflow domain.

Webb et al. (1991) and Killworth (1992) represented the FRAM velocity field by tracking the path of particles over a period of 50 days. The resulting pattern of the FRAM surface circulation shows no westward flow around Tasmania, in contradiction to our representation in Fig. 2. The most likely cause for this discrepancy is found in the initial position of the particles. No particle was released close enough to the Australian continent to resolve for the westward flow around Tasmania.

The surface circulation in FRAM is primarily wind driven. The model allows for the establishment of the subtropical gyre with a northward directed flow in the eastern Indian Ocean, but the Leeuwin Current is driven by the difference in steric height between the Pacific and Indian Ocean (Tomczak and Godfrey 1994). The exclusion of the Indonesian Throughflow domain prevents the establishment of the Leeuwin Current, which could have been generated in FRAM only through explicit forcing at the northern boundary. Although temperature values are prescribed along the northern boundary, the values are not being advected southward. The primarily wind-driven FRAM dynamics excluded the mechanism driving the Leeuwin Current.

b. Salinity

While the absent Indonesian Throughflow is the most likely cause for the observed temperature anomaly in FRAM, its absence does not explain the observed anomaly in salinity. Figure 3 shows the SSS distribution for the Levitus annual mean climatology, the FRAM data, and the difference between the two datasets. Salinities in FRAM are generally lower north of approximately 40°S and larger south of 40°S. Largest anomalies are observed again for the region west of Australia, where the climatology shows a SSS maximum. This discrepancy could not be reduced by incorporation of the Indonesian Throughflow in FRAM, since the throughflow water is fresher than south Indian Ocean surface water. Rather than increasing salinity, the inclusion of a passage would lower salinity below values already observed for FRAM and thus intensify the anomaly.

The most likely mechanism for the FRAM SSS anomalies is an overestimation of Ekman transport and the associated Ekman transport divergence in FRAM. Strong Ekman flow transports low-salinity subantarctic surface water northward, reducing FRAM SSS values in the north and in the midlatitudinal region west of Australia. The northward flow of subantarctic surface water in the Ekman layer is responsible for upwelling of NADW in the Southern Ocean, so overestimation of Ekman flow results in an overestimation of upwelling. Compared to the hydrographic properties of Southern Ocean surface water or water of the Antarctic region south of the Polar Front, NADW is characterized by both higher salinity and temperature. The increased upwelling therefore increases SSS values in the south.

Compared to the Levitus (1982) climatology, FRAM surface temperatures in higher latitudes are generally lower compared to those of subtropical and tropical latitudes, but slightly increased SST can be observed in the Antarctic Zone (Fig. 1c). The northward directed Ekman transport displaces colder water across the Antarctic Circumpolar Current (ACC) toward the temperate latitudes. An overestimated Ekman flow therefore not

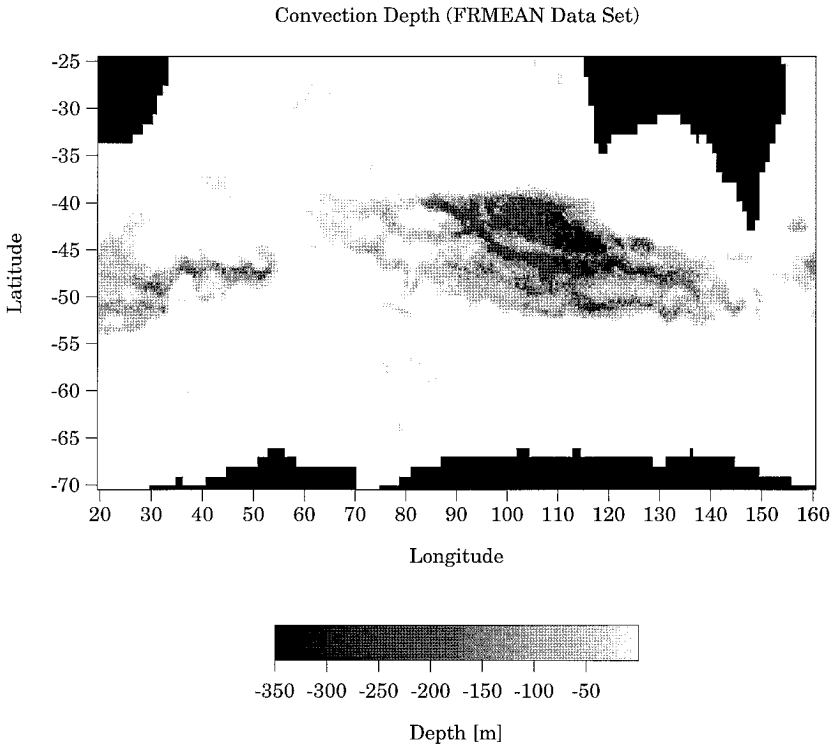

FIG. 4. Convection depth (m) in the FRAM as derived from the FRMEAN dataset density field.

only lowers salinity, but also temperature and is most likely contributing toward the temperature anomaly southwest of Australia discussed above.

It is not clear yet how well the Hellermann and Rosenstein (1983) wind stress climatology that forces the FRAM circulation represents the true winds of the Southern Hemisphere. Assuming that the winds are correct, then we see the only plausible cause for the overestimation of the Ekman transport in the FRAM and possibly in ocean circulation models in general, in the parameterization of the wind stress. According to Bye (1990), an understress τ_f generated by ocean currents counteracts the wind stress τ_w. The effective stress is then given by $\tau = \tau_w - \tau_f$. However, in FRAM only the commonly known wind stress parameterization with τ_w as given by the Hellermann and Rosenstein (1983) climatology was used. A reduction of the actual wind stress within the model by τ_f would result in a reduction of the Ekman transport and subsequent upwelling of NADW. These considerations, however, require further investigations in the future.

c. Convection

The motivation for the above analysis of SST and SSS distribution and its anomalies is a closer examination of the processes causing convection in midlatitudinal regions. The convection that is observed in a band between approximately 35° and 45°S is often thought of as being correlated with an oceanic heat loss. Hirst and Godfrey (1993) showed that at least for the domain of the Indian Ocean, the convection is dependent on the Indonesian Throughflow as well. Convection is much reduced in the no-throughflow case. Less heat is transported into the Indian Ocean; therefore, less heat is available for exchange with the atmosphere reducing surface generated convective overturn. FRAM does not include the Indonesian Throughflow, and it can be concluded that convection in FRAM in the midlatitudinal band is much reduced. FRAM convection is shown in Fig. 4 with a maximum depth of approximately 350 m, that is, bottom of model layer 8.

It is interesting to note that although the correlation of heat loss and convective overturn holds in most areas, some distinct anticorrelation is also evident. For a large region between 30° and 40°S, 90° and 110°E significant convection actually occurs in a region of oceanic heat gain (see Hirst and Godfrey 1993). In Hirst and Godfrey (1993), the deepest convection extends into layer 7, but the ocean surface exhibits a heat gain of above 40 W m^2 and should gain positive buoyancy. The location of convection in FRAM (Fig. 4) indicates that the fast northward directed transport of cold surface water due to Ekman drift (Fig. 2) constitutes a likely second mechanism for the production of negative buoyancy. The instabilities caused by an advection of denser water within the surface layer are adjusted by convection. As

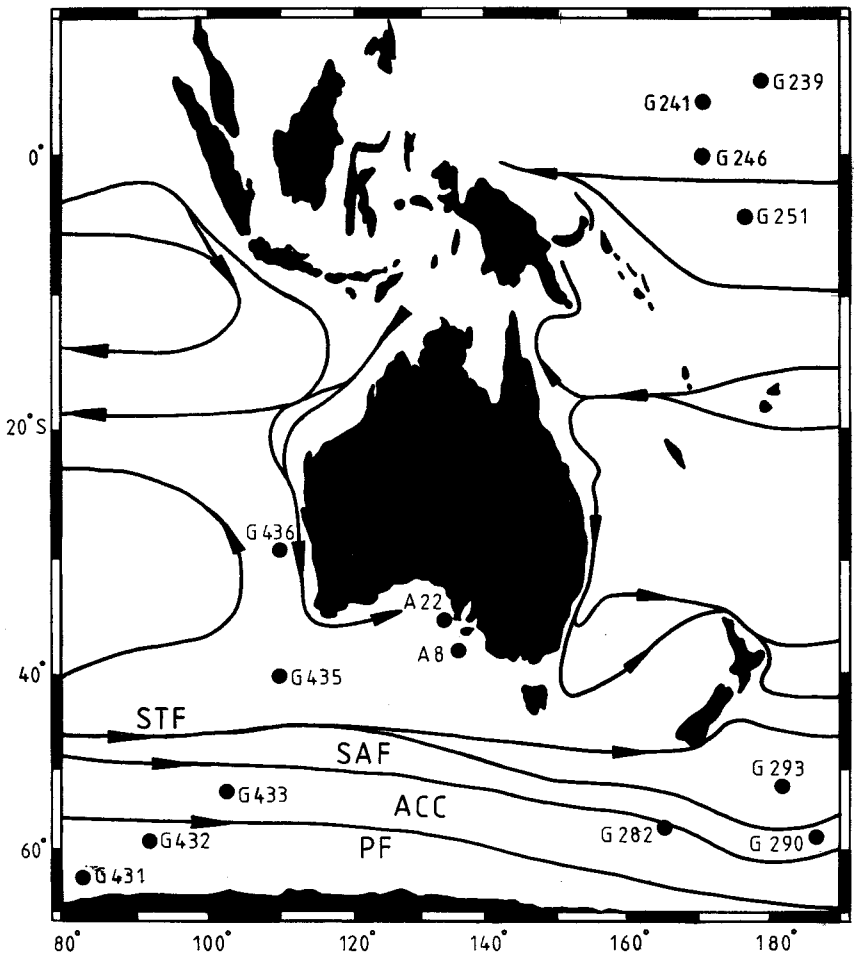

FIG. 5. Locations of stations A8 and A22 for radiocarbon analysis in the Great Australian Bight and for GEOSECS stations. The schematic representation of the oceanic circulation is taken from Tomczak and Godfrey (1994).

discussed above, the Ekman transport is most likely overestimated in FRAM. The possibility of this mechanism is, however, probably accounting for the discrepancies observed in the Hirst and Godfrey (1993) correlation of heat loss and convection.

We therefore distinguish between two possible mechanisms that cause midlatitude convection. One is due to heat loss and subsequent density increase of surface water. The second process we propose is due to a northward directed Ekman transport of subantarctic surface water across the fronts of the ACC. FRAM demonstrates reasonable convection in the midlatitudes of the southeast Indian Ocean, however, we suggest that this convection is a result of a weakened contribution of the first mechanism and an overestimation of the second process. A clarification can only be achieved in future controlled model runs allowing for variable heat and Ekman transport in the southeast Indian Ocean.

3. Discussion

The results reported by Hirst and Godfrey (1993) and the corresponding FRAM data allow us to conclude that the flow in the surface layer of the southeast Indian Ocean is not resolved correctly by FRAM. The first available radiocarbon measurements from the Great Australian Bight (Ribbe et al. 1996) support the notion of eastward surface layer flow from the Indian Ocean into the Pacific Ocean and around the southeast corner of the Australian continent. Figure 5 shows the positions of the radiocarbon profiles sampled in the Great Australian Bight with the locations of some Geochemical Ocean Section Study (GEOSECS) stations. Figure 6 compares the new measurements with the GEOSECS profiles (to a depth of 3000 m as this is the maximum vertical extent of the bight data). Oceanic radiocarbon levels are significantly determined by bomb radiocarbon that had its peak atmospheric concentration in the

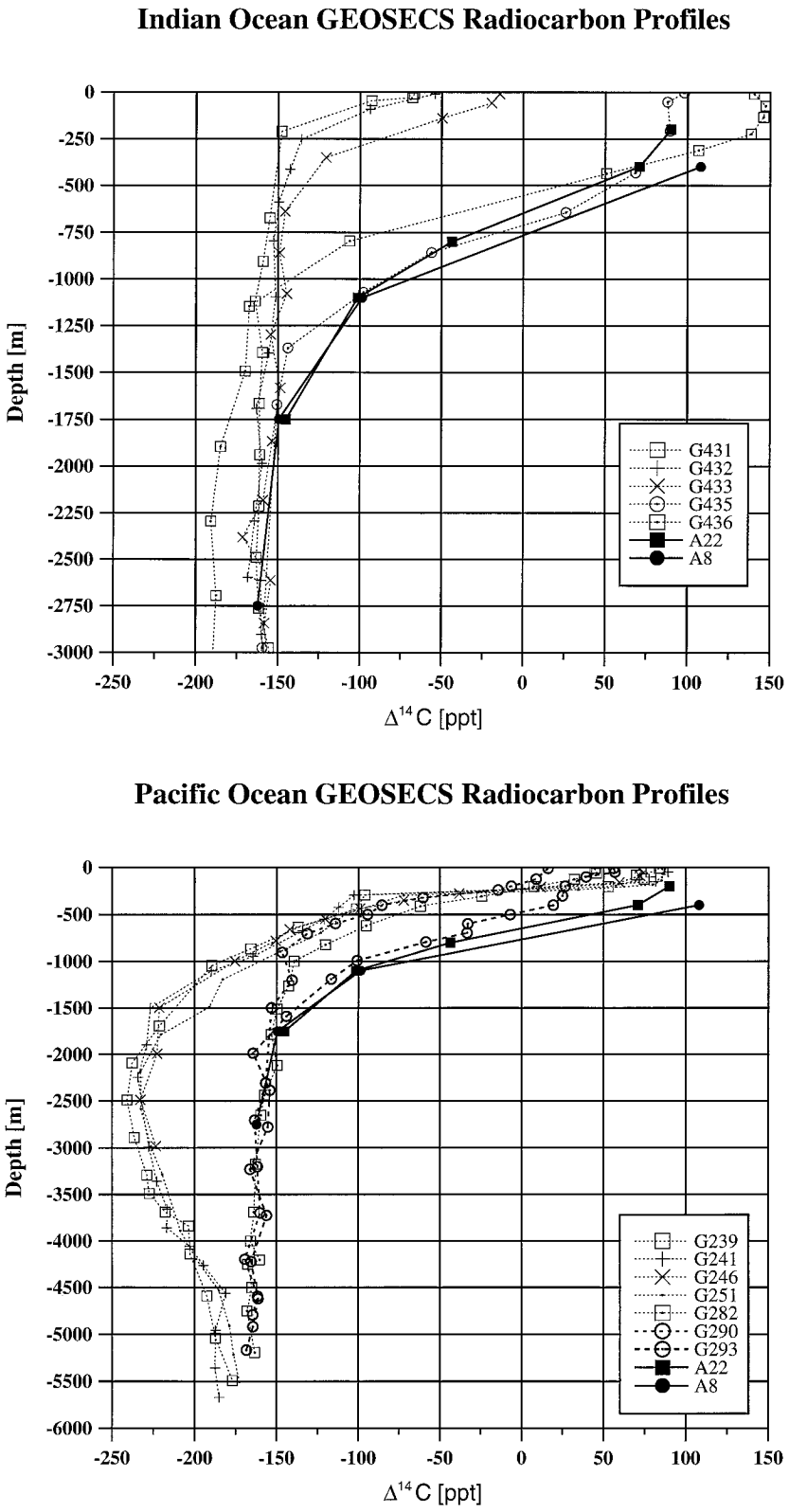

FIG. 6. A comparison of the radiocarbon observations in the Great Australian Bight with data from the GEOSECS (a) in the Indian Ocean and (b) in the Pacific Ocean. For clarity, the bight data are represented by filled symbols connected by solid lines.

Southern Hemisphere around 1965. The GEOSECS data were recorded during the 1970s (Stuiver and Östlund 1980; Stuiver and Östlund 1983), when oceanic surface concentrations of radiocarbon were most likely at or past its maximum. In a comparison of the data presented here, it is assumed that a decreased oceanic invasion rate for water of the permanent thermocline since GEOSECS in combination with downward mixing resulted in only a weak change of the surface values and slight increase within the deeper layers.

Some results obtained from the GEOSECS data and relevant to the situation in the Great Australian Bight are as follows. The GEOSECS radiocarbon inventories were high in the midlatitudinal region of the Southern Oceans and lower in the Tropics and higher latitudes (Broecker et al. 1985). Lunick (1980) presented the distribution of radiocarbon for the surface layer of the Pacific Ocean, which reflects the inventory pattern. Values of less than 100 ppt were observed west of 180°, and values between 25 and 75 ppt were reported between 10°S and 10°N. Unfortunately, no GEOSECS radiocarbon observations are available for the region of the East Australian Current (EAC) and the Tasman Sea. The EAC represents a southward extension of the Pacific Ocean's equatorial current system, which suggests that radiocarbon concentrations in the Tasman Sea are determined by equatorial values. This is supported by Lunick's (1980) interpretation of the radiocarbon database for the South Pacific Ocean in general. The Indian Ocean exhibited a specific inventory during GEOSECS approximately 25% higher than that of the Pacific Ocean (Broecker et al. 1995). The main fraction of the inventory was found in the upper 500 m of the water column, with an average penetration depth of 390 m globally. Any transport from the Pacific Ocean into the Indian Ocean either through the Indonesian Throughflow domain or south of Australia would only dilute the radiocarbon contents of the upper thermocline in the Indian Ocean and Great Australian Bight. No GEOSECS samples were collected west of approximately 180° in the Southern Hemisphere and north of the ACC, which would allow for a better comparison with our bight data.

Profiles A8 and A22 located at 38°S, 136°E and at 35.5°S, 134°E were sampled in December 1994. The sample locations are well within the domain of the negative SST anomaly observed for the FRAM data south of Australia and Tasmania. The GEOSECS profiles selected for the comparison with the bight data (Fig. 6) were chosen to be in the large-scale circulation pattern, which most likely controls the surface water characteristics of the Great Australian Bight (Fig. 5). In the upper part of the water column, only the data collected at GEOSECS station G435 in the southeast Indian Ocean are in good agreement with the data from the two Great Australian Bight stations. The sample position G435 is located at approximately 40°S, 110°E, just north of the Subtropical Front. The close similarity between the G435 and bight data is strong observational evidence that the surface waters southeast of the Australian continent are controlled by eastward flow from the Indian Ocean into the Pacific Ocean.

4. Summary

We presented evidence that FRAM may not resolve the heat flux in the southeast Indian Ocean and the flow pattern in the surface south of Australia accurately because it excludes the Indonesian Throughflow. Our argument is based upon a comparison between modeled and observed heat flux data, on new radiocarbon observations in the Great Australian Bight, and on numerical experiments reported by Hirst and Godfrey (1993).

The present analysis strongly suggests the following features for FRAM. Convection in midlatitudinal regions is too weak, upwelling in the Polar Zone is too strong, the northward Ekman transport is overestimated, and a reversed flow around the southeast corner of the Australian continent is a result of not including the Indonesian Throughflow. The analysis shows that deficiencies in FRAM are not restricted to its hydrological characteristics but also occur in aspects of its dynamics. The FRAM results demonstrate again the importance of the Indonesian Throughflow for the large-scale property distribution in the Indian and Pacific Oceans.

Analysis of more radiocarbon data from the Australian region is continuing, and results will be reported in a subsequent paper. It is expected that will strengthen the interpretation of the FRAM data of this note.

Acknowledgments. We would like to thank Dr. David Stevens for providing FRAM data and various analysis programs used for this study. Dr. Claudio Tuniz and the Australian Nuclear Science and Technology Organisation provided the radiocarbon data under AINSE Grant 94/097 (ANSTO Code OZA857U). Finally, we would like to thank Dr. J. Stuart Godfrey and an anonymous reviewer for their many comments and suggestions that improved our paper significantly. J. Ribbe acknowledges financial support through a Flinders University research scholarship and an ANSTO Special Research Grant

REFERENCES

Broecker, W. S., 1991: The great ocean conveyor belt. *Oceanography*, **4,** 79–89.

——, T.-H. Peng, G. Ostlund, and M. Stuiver, 1985: The distribution of bomb radiocarbon in the ocean. *J. Geophys. Res.*, **90,** 6953–6070.

——, S. Sutherland, and W. Smethie, 1995: Bomb radiocarbon: Separation of the natural and bomb components. *Global Biogeochem. Cycles,* **9,** 263–288.

Bye, J. A. T., 1990: Momentum coupling in ocean–atmosphere models. *J. Mar. Sys.,* **1,** 183–194.

Cai, W., and J. S. Godfrey, 1995: Surface heat flux parameterizations and the variability of thermohaline circulation. *J. Geophys. Res.,* **100** (C6), 10 679–10 692.

Döös, K., and D. J. Webb, 1994: The Deacon cell and the other meridional cells of the Southern Ocean. *J. Phys. Oceanogr.*, **24,** 429–442.

Feron, R. C. V., 1995: The Southern Ocean western boundary currents: Comparison of Fine Resolution Antarctic Model results with Geosat altimeter data. *J. Geophys. Res.,* **100**(C3), 4959–4975.

The FRAM Group, 1991: An eddy-resolving model of the Southern Ocean. *Eos, Trans. Amer. Geophys. Union,* **72,** 169–175.

Godfrey, J. S., 1996: The effect of the Indonesian Throughflow on ocean circulation and heat exchange with the atmosphere: A review. *J. Geophys. Res.*, **101**(C5), 12 217–12 237.

Grose, T. J., J. A. Johnson, and G. R. Bigg, 1995: A comparison between the FRAM (Fine Resolution Antarctic Model) results and observations in the Drake Passage. *Deep-Sea Res.*, **42,** 365–388.

Haney, R. L., 1971: Surface thermal boundary condition for ocean circulation models. *J. Phys. Oceanogr.,* **1,** 241–248.

Hellermann, S., and M. Rosenstein, 1983: Normal monthly wind stress over the world ocean with error estimates. *J. Phys. Oceanogr.,* **13,** 1093–1104.

Hirst, A. C., and J. S. Godfrey, 1993: The role of the Indonesian Throughflow in a global ocean GCM. *J. Phys. Oceanogr.,* **23,** 1057–1086.

Killworth, P. D., 1992: An equivalent-barotropic mode in the Fine Resolution Antarctic Model. *J. Phys. Oceanogr.,* **22,** 1379–1387.

Levitus, S., 1982: *Climatological Atlas of the World Ocean.* National Oceanic and Atmospheric Administration, 173 pp. and 17 microfiche.

Lunick, T. W., 1980: Bomb-produced carbon-14 in the surface waters of the Pacific Ocean. *Radiocarbon,* **22,** 599–606.

Lutjeharms, J. R. E., and D. J. Webb, 1995: Modelling the Agulhas Current system with FRAM (Fine Resolution Antarctic Model). *Deep-Sea Res.*, **42,** 523–551.

Oberhuber, J. M., 1988: An atlas based on the COADS data set: The budget of heat, buoyancy, and turbulent kinetic energy at the surface of the global ocean. Max-Planck-Institut für Meteorologie Rep. 15, 110 pp. [Available from Max-Planck-Institut für Meteorologie, Hamburg, Germany.]

Quartly, G. D., and M. A. Srokosz, 1993: Seasonal variations in the region of the Agulhas Retroflection: Studies with Geosat and FRAM. *J. Phys. Oceanogr.,* **23,** 2107–2124.

Ribbe, J., and Coauthors, 1996: First ^{14}C observations in waters of the Great Australian Bight. *Radiocarbon,* **38,** 105–106.

Rintoul, S. R., 1991: South Atlantic interbasin exchange. *J. Geophys. Res.,* **96,** 2675–2692.

Saunders, P. M., and S. R. Thompson, 1993: Transport, heat, and freshwater fluxes within a diagnostic numerical model (FRAM). *J. Phys. Oceanogr.,* **23,** 452–464.

Schmitz, W. J., Jr., 1995: On the Interbasin Thermohaline Circulation. *Rev. Geophys.*, **33**(2), 151–173.

Stevens, D. P., 1991: The open boundary condition in the United Kingdom Fine-Resolution Antarctic Model. *J. Phys. Oceanogr.*, **21,** 1494–1499.

——, and P. D. Killworth, 1992: The distribution of kinetic energy in the Southern Ocean: A comparison between observations and an eddy resolving general circulation model. *Philos. Trans. Roy. Soc. London, Ser. B,* **338,** 251–257.

——, and S. R. Thompson, 1994: The South Atlantic in the Fine-Resolution Antarctic Model. *Ann. Geophys.*, **12,** 826–839.

Stuiver, M., and H. G. Östlund, 1980: GEOSECS Pacific radiocarbon. *Radiocarbon,* **22,** 25–53.

——, and ——, 1983: GEOSECS Indian Ocean and Mediterranean radiocarbon. *Radiocarbon,* **25,** 1–29.

Thompson, S. R., 1993: Estimation of the transport of heat in the Southern Ocean using a fine-resolution numerical model. *J. Phys. Oceanogr.,* **23,** 2493–2497.

Tomczak, M., and J. S. Godfrey, 1994: *Regional Oceanography: An Introduction.* Pergamon, 422 pp.

Wadley, M. R., and G. R. Bigg, 1994: Interbasin exchange of bottom water in ocean general circulation models. *J. Phys. Oceanogr.,* **24,** 2209–2214.

Webb, D. J., P. D. Killworth, A. C. Coward, and S. R. Thompson, 1991: *The FRAM Atlas of the Southern Ocean.* Natural Environment Research Council, 67 pp.